Simulation of the hone broaching process with diamond tools

Guilherme Evangelista Vargas, Konrad Wegener, Friedrich Kuster & Rolf Bertrand Schroeter

Journal of the Brazilian Society of Mechanical Sciences and Engineering

ISSN 1678-5878
Volume 36
Number 2

J Braz. Soc. Mech. Sci. Eng. (2014)
36:325-333
DOI 10.1007/s40430-013-0085-z

Springer

Your article is protected by copyright and all rights are held exclusively by The Brazilian Society of Mechanical Sciences and Engineering. This e-offprint is for personal use only and shall not be self-archived in electronic repositories. If you wish to self-archive your article, please use the accepted manuscript version for posting on your own website. You may further deposit the accepted manuscript version in any repository, provided it is only made publicly available 12 months after official publication or later and provided acknowledgement is given to the original source of publication and a link is inserted to the published article on Springer's website. The link must be accompanied by the following text: "The final publication is available at link.springer.com".

Author's personal copy

J Braz. Soc. Mech. Sci. Eng. (2014) 36:325–333
DOI 10.1007/s40430-013-0085-z

TECHNICAL PAPER

Simulation of the hone broaching process with diamond tools

Guilherme Evangelista Vargas · Konrad Wegener · Friedrich Kuster · Rolf Bertrand Schroeter

Received: 15 July 2012 / Accepted: 20 June 2013 / Published online: 22 August 2013
© The Brazilian Society of Mechanical Sciences and Engineering 2013

Abstract Hone broaching is a finishing process characterized by an oscillatory movement of the single layer diamond tool. The tool consists of a conical roughing and a cylindrical finishing part. The finishing part increases the surface quality and reduces the tolerances. To reach a deeper understanding of the process, a stochastic model of the cutting tool was developed. It allows the examination of the influence of different process and tool parameters by numeric simulation based on the investigation of chip formation. Therefore, the simulation reproduces the macroscopic effects of the hone broaching process based on the fundamental microscopic description of single grains and their cutting edges' engagements. The model-based analysis showed several suggestions for the improvement and optimization of the hone broaching process, which have been experimentally verified in this work. With a modified oscillatory strategy, a considerable process time reduction can be achieved.

Technical Editor: Alexandre Abrão.

G. E. Vargas (✉)
Maag Pump Systems AG, 8154 Oberglatt, Switzerland
e-mail: GuilhermeVargas@maag.com

K. Wegener · F. Kuster
Swiss Federal Institute of Technology Zurich, Institute of Machine Tools and Manufacturing, 8092 Zurich, Switzerland
e-mail: wegener@iwf.mavt.ethz.ch

F. Kuster
e-mail: kuster@iwf.mavt.ethz.ch

R. B. Schroeter
Laboratory of Precision Mechanics, Federal University of Santa Catarina, Florianópolis, SC 88040-900, Brazil
e-mail: rolf@emc.ufsc.br

Keywords Hone broaching · Hard broaching · Modeling · Simulation · Cutting forces

List of symbols

$1-m_c$	Specific cutting force, N/mm^2
3D	Three-dimensional, dimensionless
A	Cutting area, mm^2
a_{side}	Length of the cube, mm
b	Cutting width, mm
CBN	Cubic boron nitride, dimensionless
D	Diamond, dimensionless
F_c	Cutting force, N
F_{cN}	Cutting perpendicular force, N
FEM	Finite element method, dimensionless
f_k	Feed per grain, mm
f_{stroke}	Feed per stroke, mm
f_z	Feed per tooth, mm
h	Cutting depth, mm
h_{corner}	Distance from the surface of the octahedron to its neighboring cube corner, mm
HRC	Hardness measurement in Rockwell scale C, dimensionless
ISO	International organization of standardization, dimensionless
$k_{c\mu.\mu}$	Specific cutting force evaluated for a cutting depth and cutting width of 1 μm, N/mm^2
t	Pitch, mm
v_c	Cutting speed, m/s

Greek symbols

$\triangle l$	Change of length, mm
μ	Cutting force ratio, dimensionless
ξ	Variable to characterize the theoretical crystal morphology of diamonds, dimensionless
v	Rotation angle around the y-axis, deg

Author's personal copy

φ Rotation angle around the x-axis, deg
ψ Rotation angle around the z-axis, deg

1 Introduction

Hone broaching, commonly named "hard broaching" by the industry, is a finishing process developed in the 1990s to correct geometrical deviations of inner profiles on hardened workpieces. The process is applied in workpieces with any type of inner profile, for example, in the involute gear manufacturing for cars, motorcycles or trucks gearboxes. After the hardening process, the workpieces show hardening distortions and geometric failures which bring them outside the tolerance zone. The hone broaching can be applied to bring these workpieces back into the tolerance zone, thus avoiding their rejection and additionally improving their surface quality [1].

Since most of the workpieces being machined have high hardness (usually above 60 HRC), the application of special tools is required. The hone broaching tool differs from the conventional broaching tool by the application of diamond grains distributed stochastically on the surface as cutting edges. Both tools consist of a conical part for material removal and a cylindrical part for finishing the workpiece surface to its final quality. The outer contour of the tool has the negative form of the profile being machined and must be adapted to the geometry of the workpiece [1–3]. With a conventional broaching tool, the feed per tooth f_z is determined by the conicity of the conical part and the pitch t, which represents the distance between two cutting edges [4]. The same applies to hone broaching tools—the feed per grain f_k is determined by the conicity and the grain density (Fig. 1). Since the grain size and the distance between two grains are stochastic variables and can only be statistically determined, an accurate feed per grain f_k cannot be determined and, thus, this parameter can only be defined statistically.

Hardened materials up to 62HRC can also be machined using conventional broaching tools. Thereby hard metal broaching tools used in the industry and cubic boron nitride (CBN) tools are applied in laboratory tests. Due to the high costs associated with tool manufacturing and preparing, the process can only be effectively used in mass production [4–7].

Similarly to the broaching process, hard fine gear shaping also offers the option to manufacture hardened internal gears. However, since very low quantities per tool are produced, this process cannot be economically used in the series production [8].

Modeling and simulation of an abrasive process is used for the better understanding of the process and also for its optimization, and plays an important role in predicting forces and deformations during the cutting process. Zitt and Warnecke [9] and Zitt [10] have developed a geometric-kinematic model of the grinding process in which three-dimensional abrasive grains are created and the interaction of each individual grain is observed and considered. The cutting forces calculation is carried out by a balance between the sum of the cutting surfaces obtained from the simulation and the cutting forces measured in experiments. Nevertheless, with this method no distinction is made as to whether the sum of the cutting surfaces used in the simulation is obtained from many small or few large cutting edges. Pinto [11] proposed an analogy to Kienzle equation to calculate the cutting forces in his geometric-kinematic simulation of brazed and electroplated grinding wheel with defined grain arrangement. In his model, the specific cutting force of each grain is taken into account as a function of the respective cutting surface, determining the relationship between forces and surface by comparison between measurements and simulation.

In this work, a stochastic process model is presented as a support to understand the physical process taking into account the stochastic nature of the tool and the process. The theoretical foundation of the hone broaching was developed for the modeling and process simulation, identifying and investigating the effects of process parameters and tool data on the forces, the achievable surface quality and accuracy of the workpiece. The model includes the

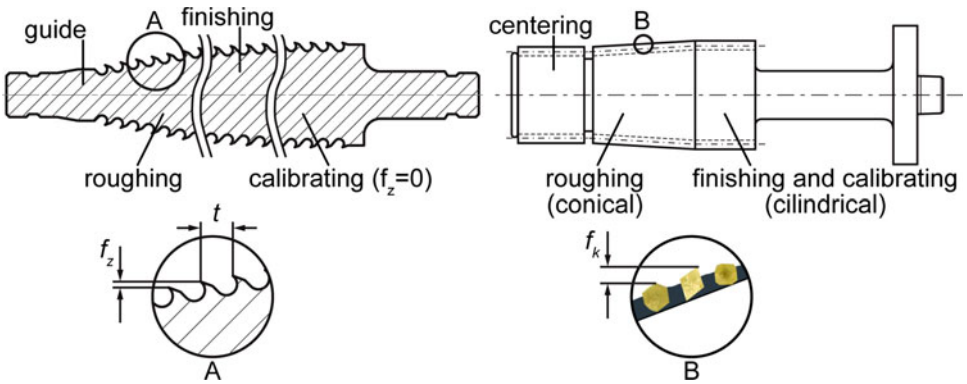

Fig. 1 Conventional broaching tool (*l*) [2] and hone broaching tool (*r*) [1]

Author's personal copy

microscopic properties of the abrasive grain through a detailed description of the morphology and the macroscopic characteristics of the process kinematics between tool and workpiece. The prediction of the occurring process forces in the model considers the chip formation mechanisms of a single grain, which was investigated by single grains experiments [12, 13].

2 Oscillatory strategy

During the hone broaching process, the workpiece is machined by the axial oscillating motion of the tool. At each stroke the tool moves deeper into the workpiece, until the entire profile is processed. The oscillatory motion lowers the cutting forces in the process, reducing tool wear and, thus, leading to an increased tool life. Besides that, shorter tools can be made using an oscillatory strategy. This leads to a reduction of production expenses and costs related to production time, which increases the efficiency of the process [12].

The oscillatory motion in the hone broaching process occurs between the starting and final position of the tool (Fig. 2). The starting position is defined in a way that the beginning of the conical part of the abrasive layer and the center of the oil nozzle are on the same level in the cutting direction. The final position of the hone broaching movement is reached when $\sim$3 mm of the rear cylindrical part of the tool is still in contact with the workpiece.

Between the starting and the final position, numerous successive upward and downward strokes are made. With each upward stroke, the position is increased by a constant amount (referred to as feed-per-stroke f_{stroke}) until the final position is reached. The upward strokes are responsible for the material removal. Each upward stroke is followed by the retraction to the level of the oil nozzle. The retreat serves to clean the chipping from the tool and happens only up to the line of the tool, which is still in contact with the workpiece. As soon as the final position is reached, additional calibrating strokes give the workpiece its final dimensions and quality. In addition, during this phase, due to the elasticity of tool and workpiece, small chippings are removed by each up-and-down movement. These chippings are stored in the chip space in the abrasive layer and must be removed after each stroke.

3 Simulation of the hone broaching process

The simulation of the hone broaching process is based on the stochastic description of the tool abrasive pad, using the grain size, morphology, location and orientation of the randomly simulated diamonds on the surface of the tool body. It is based on a kinematic-geometrical model and consists of six sub-models: tool, kinematic process, material removal, force, deformation and chip space model. The tool model is based on the Monte Carlo method and considers the most important variables of the abrasive surface. The kinematic process model is based on the motion of the tool and corresponds to that of the oscillatory hone broaching strategy. The material removal model assumes a kinematic cutting condition. The force model is based on the Kienzle force model for a single grain, while the elasticity of the workpiece is considered in the deformation model. The chip space model takes into account the relationship between the chip volume and the chip space. The model allows the mapping of the macroscopic effects of the process, starting with the careful and basic description of the microscopic properties of individual grain intervention.

3.1 Tool model

The tool model is based on the Monte Carlo simulation and consists of a detailed description of the macro- and micro-geometry of the tool. The macro-geometry is described by the length of the conical and the cylindrical part, the

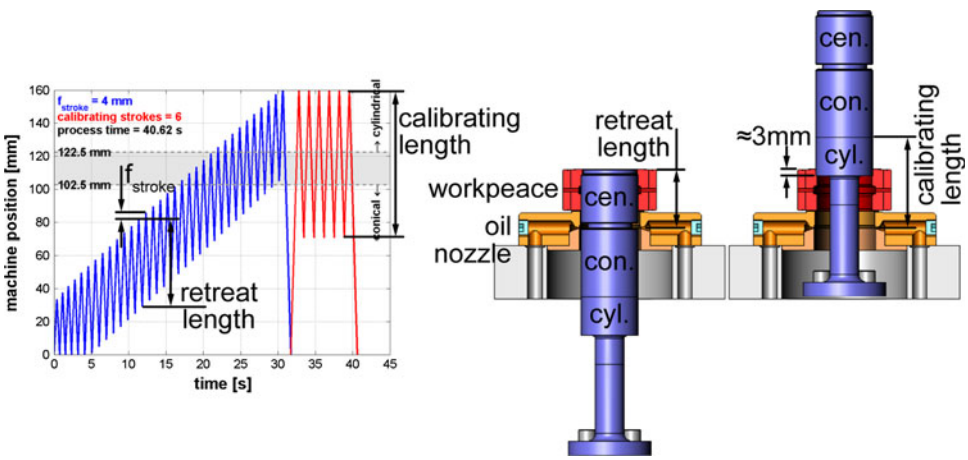

Fig. 2 Definition of starting (l) and final position (r) in hone broaching [14]

Author's personal copy

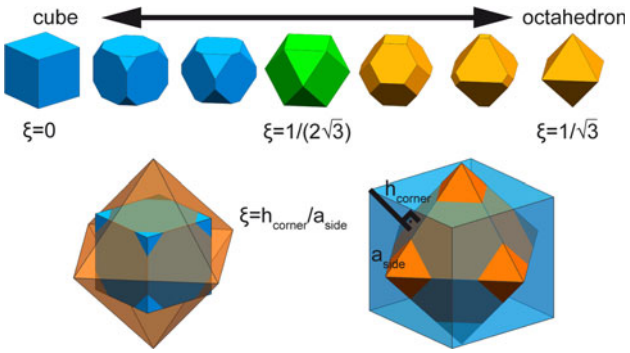

Fig. 3 Theoretical crystal morphology of synthetic diamond [18]

conical shape and the geometry of the inner profile. Form and position deviations are not included in the model.

The micro-geometry refers to the abrasive used. Diamond is mainly used as cutting tool material in the hone broaching process. To characterize each individual grain, the theoretical crystal morphology of synthetic diamond is used (Fig. 3). This may vary continuously from the shape of a cube to an octahedron [15–17]. To determine and to use an exact morphology for the simulation, a dimensionless variable ξ has been introduced [18]. This variable is the ratio between the distance from the surface of the octahedron to its neighboring cube corner (h_{corner} in Fig. 3) and the side length of the cube (a_{side} in Fig. 3). Thus, all theoretical crystal morphologies of the diamond can continuously be represented by shapes varying from a cube ($\xi = 0$) to an octahedron ($\xi = 1/\sqrt{3}$).

The grain size is characterized by the ISO 6106 [19]. The standard describes the grain within two limits, which are indicated by the size of the test sieves. However, no information on allocation and characterization of the variation between these two limits is provided. The characterization of the variable ξ and the grains is experimentally determined for the diamond grains used in the hone broaching. The variable ξ can be presented with sufficient accuracy by a normal distribution with mean 0.41 and standard deviation 0.05. As well, the grain D126 can be approximated to a normal distribution with a mean of 123 μm and a standard deviation of 18 μm and is bounded between the upper and lower test sieve [18].

After the grains generation they can be rotated around the three orientation angles φ, ψ and υ. It is supposed that each grain can assume arbitrary values for these orientation angles. Each angle determination occurs stochastically by a uniform distribution, which may be any angle between 0° and 360°, and then they are distributed to the main body of the tool. To allow a realistic distribution, the position of the grains from a total of 80 samples covering an area of 1 mm^2 was evaluated under a microscope. These many patterns are stochastically chosen and the grains position

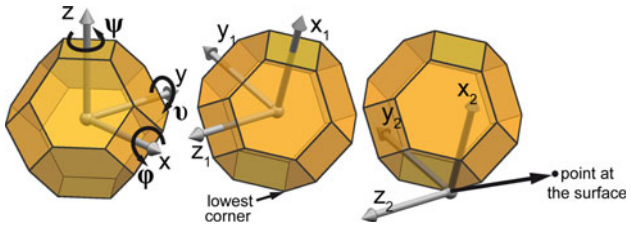

Fig. 4 Position and orientation of the grains

on the base surface is given according to this pattern. Here, the grain with the deepest corner in relation to the Z values is selected as the reference point (Fig. 4).

The virtual image of the hone broaching tool results from the stochastic generation of the grain morphology, grain size, grain orientation and grain position.

3.2 Material removal model

Due to the complex mechanism of chip formation, all thermal, mechanical and chemical relationships cannot be considered in a single model. Therefore, some assumptions and simplifications are made in the modeling of the material removal. It is assumed that the material removal can be reduced to a kinematic analysis of the process. The real cutting process is simplified using only a kinematic interface condition that is considered ideal. Elastic and plastic micro deformations, burrs and thermal effects are neglected in the model. With these simplifications, the cutting operation is reduced to a geometric interaction between grain and workpiece [11, 18]. The result is a groove on the workpiece surface as a negative image of the profile of abrasive (Fig. 5). The interaction surface A between the workpiece and the diamond grain is assumed being the cutting area of this grain.

The simplifications described above lead to the fact that only the 3D geometry is needed for the grain contour generation. The full 3D information of all grains is not necessary for the other models. Therefore, a simplification of the 3D grain geometry is accomplished by reducing the grain projection to a plane perpendicular to the cutting direction [11, 18]. This simplification is shown in Fig. 6.

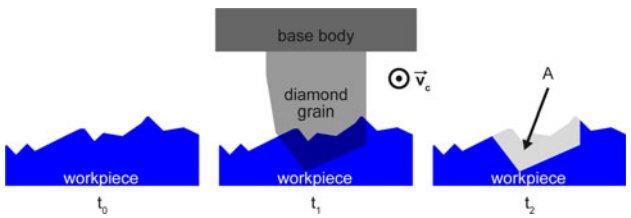

Fig. 5 Model of material removal [18]

Author's personal copy

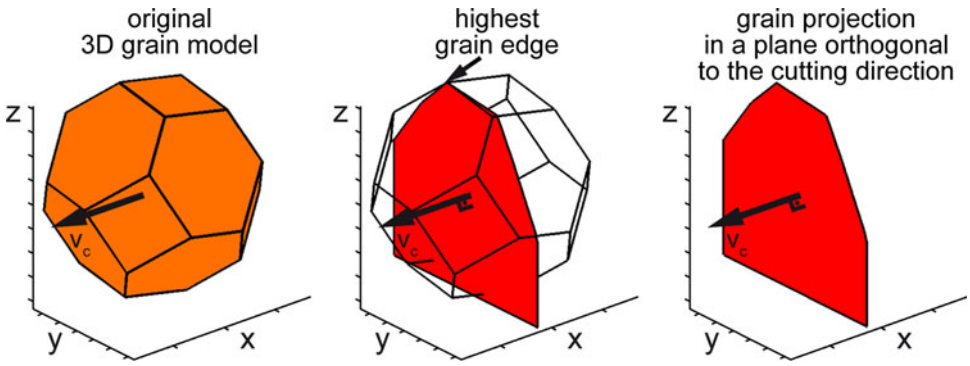

Fig. 6 Simplification of 3D geometry

The position of the grain projection is determined by the highest cutting edge of the grain. To calculate the cutting force in the force model, the depth and width of the cut surface are needed. However, a direct determination of the width and depth is not possible, because the shape of the interaction surface is not uniform. It is assumed in this work that the cutting width b corresponds to the distance between the two extremes of the cutting area A (Fig. 5). With the cutting area A and the average width b, an average cutting depth h is calculated by:

$$h = {}^{A}/_{b} \tag{1}$$

The elastic deformation of the workpiece has to be considered in the simulation (Fig. 7). This is estimated before the engagement surfaces calculation and in the form of an offset account of the workpiece profile.

After the estimation, the cutting surfaces of all active grains are calculated. These are then used to calculate the cutting forces and deformations. The calculated deformation is then compared with the estimated value. The difference between estimated and calculated deformation should lie within a specified tolerance. If this is not the case, the process is repeated with a new estimation until the error between estimated and calculated deformation is minimized.

The engagement surfaces of all active grains are used to calculate in one step the forces acting on the force model.

3.3 Force model

Using the model, the cutting perpendicular force and cutting force are calculated from the upward strokes. Here, the microscopic properties of the individual grain are considered by the calculation of the forces of a single grain. The intervention of each grain results in a component of force F_{ci} in the cutting direction, which is the product of the average width b_i, the cut depth h_i elevated by the exponent of the specific cutting force $1-m_c$ and the specific cutting force $k_{c\mu.\mu}$. This results in the Kienzle equation for calculating the cutting force as a function of average width and depth:

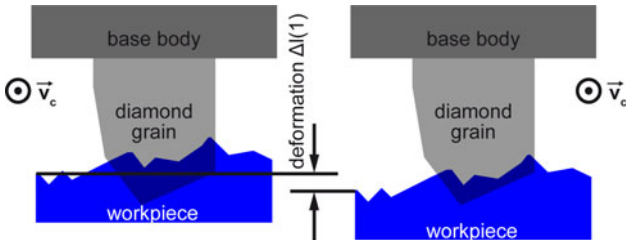

Fig. 7 Material removal model without (*left*) and with (*right*) taking the deformation into account

$$F_{c\,i} = k_{c\,\mu.\mu} \cdot b_i \cdot h_i^{1-m_c} \tag{2}$$

The values for $k_{c\mu.\mu}$ and m_c were taken from single grain experiments. The preliminary study of the influence of grain orientation on the chip formation mechanism at low cutting speed is presented in former publications [12, 13]. A more comprehensive analysis is in course and will be the focus of a future publication.

The effective cutting force F_c is calculated from the sum of the individual force components of all active grains.

$$F_c = \sum_i F_{c\,i} \tag{3}$$

The force component perpendicular to the cutting direction F_{cNi} results from the cutting force ratio μ:

$$F_{cN\,i} = {}^{F_{c\,i}}/_{\mu} \tag{4}$$

The cutting force ratio μ is determined experimentally and results from the quotient between the cutting force and the average cutting perpendicular force (F_c/F_{cN}). The conical part of the tool is responsible for the material removal. During contact between the workpiece and the conical part of the covering, the ratio on average amounts to $\mu = 0.25$. The cylindrical part ensures the quality of the workpiece. In order to achieve a reduced workpiece roughness, the grains are dressed in this area. By dressing the diamond grains the highest peaks were deliberately blunted, so that the grain peaks are smoothed. This blunting results in a decrease of cutting force ratio. Once contact occurs only with the cylindrical

Author's personal copy

part, the cutting force ratio on average amounts to $\mu = 0.15$.

In the simulation, the position of the active grains is being analyzed and the corresponding average cutting force ratio of 0.25 is assumed for the conical and of 0.15 for the cylindrical part.

Analogous to the cutting force, the average cutting perpendicular force F_{cN} is the resultant of the sum of the individual force components in the interface perpendicular direction:

$$F_{cN} = \sum_i F_{cN\,i} \tag{5}$$

The deformation is calculated with the average cutting perpendicular force.

3.4 Deformation model

The interaction between grain and workpiece causes a force, consequently deforming the workpiece. In a finite element method (FEM) simulation, the calculation of strength and deformation occurs by solving a linear system of equations [20]. In order to observe the deformations, an alternative method is used. Instead of solving a system of equations, the elastic deformation of the workpiece is estimated before the calculation of the engagement surfaces. This estimated deformation is then considered for the determination of the cutting surfaces of all the active grains, and after that the forces in the force model can be determined. Hence, the elastic deformation is calculated taking into account the real deformation curve of the workpiece. This curve is obtained by FEM simulation considering the geometry of the workpiece and the material properties. In the modeling, a linear relationship between force and deformation is assumed. This results in the change of length Δl as a function of the average cutting perpendicular force F_{cN}:

$$\Delta l = 37.2 \cdot 10^{-3} \cdot F_{cN} \tag{6}$$

The final objective is to obtain the estimated elastic deformation consistent with the calculated value. If the error between estimated and calculated deformation is outside a specified tolerance, a new value is estimated for the deformation and the process of material removal model over the force model is repeated until the deformation model is within an acceptable precision level. This iterative process is repeated several times until the error is minimized. Only then can a new step of the upstroke be simulated.

3.5 Chip space model

One of the most influential parameters of hone broaching is the feed per stroke. An increase of feed per stroke leads to a substantial reduction in processing time, which can positively affect the economics of the process. Nevertheless, the boundaries and impact on the tool life is unknown. With greater feed per stroke, a higher volume of chips is removed, and the chip space existent in the layer must carry these chips. If the feed is too low, the chip space is not fully utilized. On the other hand, with too large a feed the chip space can be jammed up, which can increase the wear on the tool and shorten the tool life considerably. Thus, there is an optimum value of feed per stroke, workpiece height and grain size and form in which there is no blockage, the maximum material removal occurs and the layer wear is low. However, the determination of this optimum requires a very complex investigation, which only with great effort is experimentally possible. For this reason, the ratio of the volume of the removed chip and the chip space is determined using the simulation.

In the literature, the chip space is often regarded in two dimensions and thereby assumed to include only the volume directly in front of the abrasive grain in the cutting direction. As can be seen in Fig. 8, left, the chips store not only before but also around the active grain. Depending on the process parameters, the chip volume can be so large that the entire region surrounding the grain is completely filled with chips.

It was also found that the chips mostly fill the spaces that are limited by the neighborhood. Rarely was a chip found, which had exceeded the boundaries of neighboring grains, as shown in Fig. 8 on the right.

In this work, the chip space is defined as the free volume around the corner of the active cutting grain, limited by its direct neighboring grains.

The chip space model is simulated after each upward stroke, after all active grains and their associated sectional area were evaluated in a single stroke. Here, the direct neighbors of each active grain are identified and the volume of each of these grains is calculated. Only the portion of the grain, which is above the bond, is considered (Fig. 9). From the outside contour of the active grain and its neighbors, the convex hull is calculated. The chip space arises from the difference between this volume and the volume of the considered grain.

The distribution of the chip spaces in an upward direction results from the calculation of the chip space of all active grains. In addition, the ratio of the volume of removed chips is calculated for the corresponding chip space. It is assumed that the coolant can flow away in the chip space and, thus, the chip space is filled only by chips. From this, the percentage of chip-filled areas in chip space in the upward stroke can be determined.

Author's personal copy

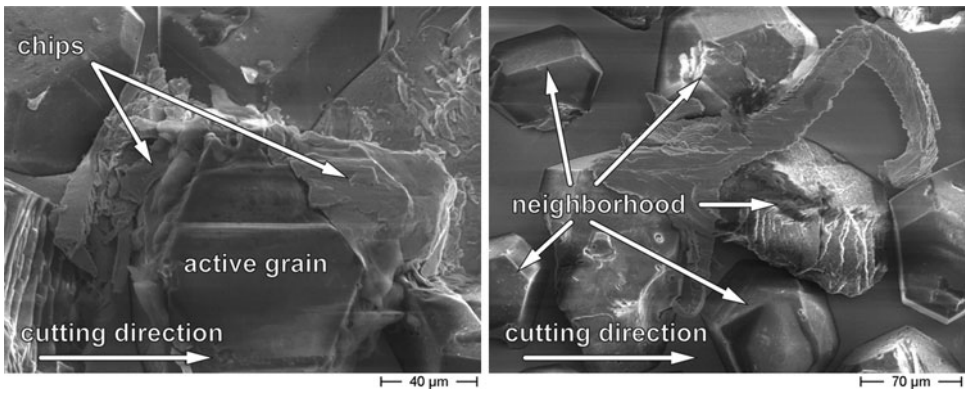

Fig. 8 Deposition of chips around the active grain

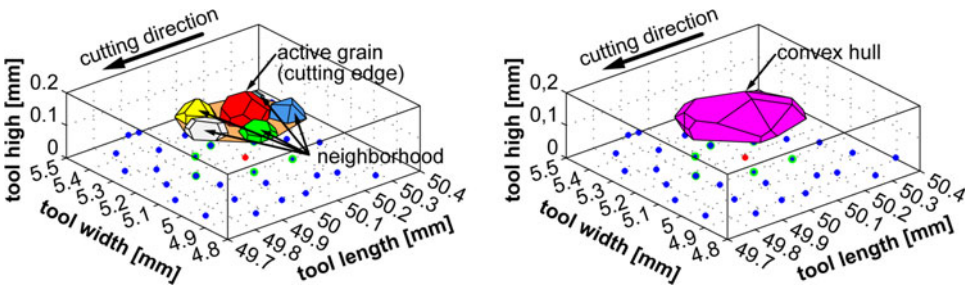

Fig. 9 Identification of the active grains and the neighborhood (*left*) and calculation of the convex hull (*right*)

Table 1 Simulations parameters

Process parameter		Tool parameter	
Cutting speed	180 mm/s	Grain	D126
Start position	SP = 20 mm	Length of conical part	70 mm
Hone broaching strategy	P1 = 138 mm	Length of cylindrical part	40 mm
Feed per stroke	f_{stroke} = 2.5 mm, 5 mm and 7.5 mm	Conicity	1/1000
Forward strategy	S2	Workpiece parameter	
End position	EP = 177 mm	Workpiece height	20 mm
Finishing length	LS = 105 mm	Workpiece width	5 mm
Number of finishing strokes	$n = 1$	Desired removal	50 µm
Step length (upward strokes)	5 mm	Distance between workpiece planes	2.5 mm

3.6 Model verification

For the model verification, simulations are performed with the same process parameters as they were used in the hone broaching experiments. Table 1 provides a summary of these parameters.

To calculate the cutting force, the microscopic properties of individual grain interaction will be considered. In the preliminary experiments with single grains presented in Vargas [12], the values of $k_{c\mu.\mu}$ and m_c varied according to the grain orientation. Due to the high complexity, the grains orientation will be neglected here. A preliminary investigation has shown that the results from the force model with the values of $k_{c\mu.\mu} = 0.041$ N/µm^2 and $m_c = 0.452$ [12] correlate well with the measured values, and it can be seen that the mathematically identified parameters are not far away from any physical reality. To calculate the cutting perpendicular force, a cutting force ratio of 0.25 is assumed for the conical, and 0.15 for the cylindrical part. The deformation curve corresponds to that of Eq. 6.

The effect of the cutting speed v_c and the feed per stroke f_{stroke} on the forces was investigated by Vargas [14]. No effect of the cutting speed on the forces was detected within the analyzed parameter window, as the machine is limited to a maximal cutting speed of 220 mm/s (13.2 m/min). Unlike the cutting speed, the feed per stroke f_{stroke} presented a considerable effect on both cutting and perpendicular cutting forces. Therefore, the model verification

Author's personal copy

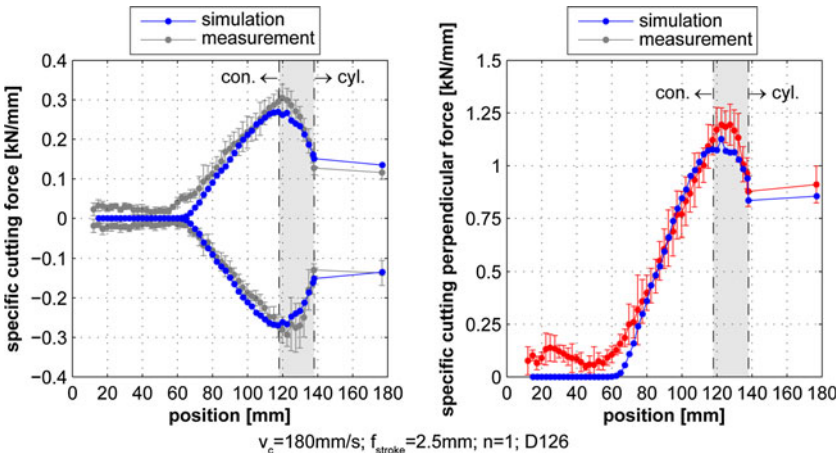

Fig. 10 Comparison of forces between simulation and experiment for $f_{\text{stroke}} = 2.5$ mm

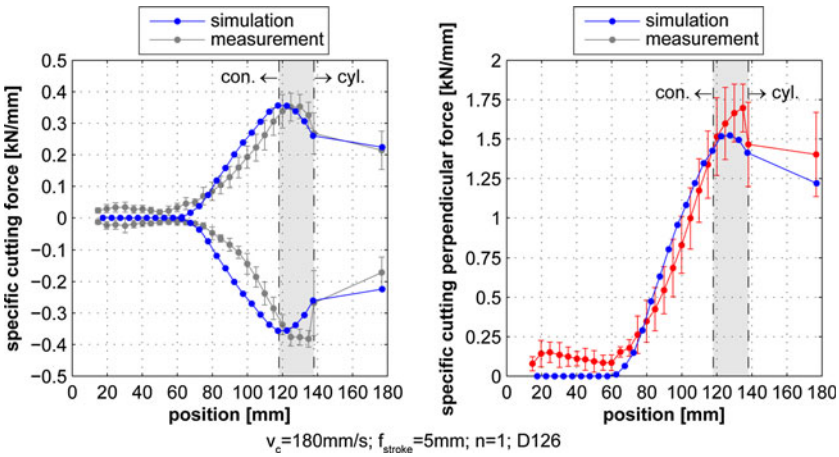

Fig. 11 Comparison of forces between simulation and experiment for $f_{\text{stroke}} = 5$ mm

was carried out only for a cutting speed of 180 mm/s for different values of feed per stroke f_{stroke} (Table 1).

In all simulations a good correlation between experiment and simulation of forces is achieved, as can be seen in the examples presented in Figs. 10 and 11 for the comparisons between simulation and experiment for feed per stroke of 2.5 and 5 mm. Virtually, all simulated values are within range of the measured dispersion with a 95 % confidence interval.

The simulation results are consistent with the measured values not only for the process forces, but also for the mutually independent variable roughness and material removal. Thus, the assumptions for the simulation are accurate and the representation of the hone broaching process starting from the description of the abrasive layer up to the microscopic properties of each individual grain is assured.

4 Summary

In this work, a simulation based on a kinematic-geometric process model was developed and validated, with which the impact of changes in the process parameters and tool data can be studied by numerical simulation. As input data the geometry of tool and workpiece, the grain and the process parameters are used. The simulation allows the mapping of the macroscopic effects of the process based on the complete and fundamental description of the microscopic properties of individual grain intervention. Thus, the forces and the resulting deformations can be calculated. This is very useful for a specific design of the tool, so that from the beginning the results are already within the tolerance limit.

In the validation, the geometry of the workpiece was limited to plane and cylindrical surface. However, an extension of the model to internal gears would be useful for its industrial use. Although the D126 grade is mainly applied in the hone broaching process, the model should also be extended to other grades. This allows new applications for the simulation.

Acknowledgments The authors would like to thank the project partners, Fässler AG, Breu Diamantwerkzeug GmbH and Kistler Instrumente AG, for their support for this project. This project was funded by the Innovation Promotion Agency KTI in Switzerland. The corresponding author carried out the presented work during his time as research associate at inspire AG/IWF.

Author's personal copy

References

1. Gerber M (2000) Harträumen von Innenprofilen mit Diamantwerkzeugen. Feinbearbeitung von Zahnrädern, Aachen, pp 10–17
2. Klinger M (1993) "Räumen gehärteter Innenprofile". Heft 398. Forschungsvereinigung Antriebstechnik e.v, Frankfurt
3. Kallabis M (1991) Räumen gehärteter Werkstoffe mit kristallinen Hartstoffen. Universität Karlsruhe, Dissertation
4. Klocke F, König W (2008) Fertigungsverfahren 1—Drehen, Fräsen, Bohren, 8th edn. Springer, Berlin
5. Klocke F, Brinksmeier E, Weinert K (2005) Capability profile of hard cutting and grinding processes. CIRP Annals Manuf Technol 54(2):22–45
6. Schmidt J, Lang H (2003) "Harträumen stösst mit CBN in neue Dimensionen vor", Werkstatt + Betrieb pp 9:50–52
7. Lang H (2003) Harträumen mit CBN—Grundlagenforschung für die Zukunft. Karlsruher Kolloquium, Karlsruhe, pp 61–73
8. Mehr A (2004) Hartfeinbearbeitung von Verzahnungen mit kristallinen diamantbeschichteten Werkzeugen beim Fertigungsverfahren Wälzstossen. Universität Karlsruhe, Dissertation
9. Warnecke G, Zitt U (1998) Kinematic simulation for analyzing and predicting high-performance grinding processes. CIRP Annals Manuf Technol 47(1):265–270
10. Zitt UR (1999) Modellierung und Simulation von Hochleistungsschleifprozessen. Universität Kaiserslautern, Dissertation
11. Pinto FW, Vargas GE, Wegener K (2008) Simulation for optimizing grain pattern on engineered grinding tools. CIRP Annals Manuf Technol 57(1):353–356
12. Vargas GE (2010) Analyse und Simulation des Prozesses Honräumen von gehärteten Innenprofilen mit Diamantwerkzeugen. Dissertation, ETH-Zurich
13. Wegener K, Vargas GE, Wunder S, Kuster F, Pinto FW (2008) "An experimental approach for grain wear for improving kinematic–geometrical simulation", In: euspen International Conference, Zurich-Switzerland, 1:130–134
14. Vargas GE, Wegener K, Kuster F, Schnider T (2008) Analysis and optimisation of the hard broaching process with diamond tools. Int J Mecha Manuf Sys 1(4):365–376
15. Field JE (1992) The properties of natural and synthetic diamond. Academic Press, London
16. Bailey MW, Hedges LK (1995) Die Kristallmorphologie von Diamant und ABN. Industrie Diamanten Rundschau 29(3): 126–129
17. Bailey MW, Hedges LK (1995) Crystal morphology identification of diamond and ABN. Ind Diamond Rev 55(1):11–14
18. Wegener K, Vargas GE, Kuster F, Pinto FW, Schnider T (2008) "Modelling of hard broaching", In: Proceedings of the 9th Biennial Conference on Engineering Systems Design and Analysis, Haifa-Israel, pp 427–435
19. ISO 6106:2005(E), Abrasive products–checking the grit size of superabrasives
20. Brinksmeier E, Aurich JC, Govekar E, Heinzel C, Hoffmeister HW, Klocke F, Peters J, Rentsch R, Stephenson DJ, Uhlmann E, Weinert K, Wittmann M (2006) Advances in modeling and simulation of grinding processes. CIRP Annals Manuf Technol 55(2):667–696